Stroke

BASIC AND TRANSITIONAL SCIENCES

Spatial Proteomics Analysis of Soft and Stiff Regions in Human Acute Arterial Thrombus

Hongcheng Mai, MD*; Tianyuan Zhang, MD*; Tao Zhang, MD, PhD*; Aijun Lu, MD; Zhengdong Wu, MD; Bing Yang, MD; Niu He, MSc; Xiaoyan Liu, MD, PhD; Chi Kwan Tsang, PhD; Anding Xu, MD, PhD; Dan Lu, MD, PhD

BACKGROUND: The soft regions of a thrombus tend to be more susceptible to r-tPA (recombinant tissue-type plasminogen activator)-mediated thrombolysis and are more easily removed by mechanical thrombectomy than the stiff counterpart. This study aimed to understand the molecular pathological differences between the soft and stiff regions of human arterial thrombus.

METHODS: We developed a spatial proteomic workflow combining proteomics with laser-captured microdissection to analyze human arterial thrombi with Masson trichrome staining to identify stiff and soft regions from 2 independent cohorts of patients with acute myocardial or cerebral infarction. Dysregulated proteins in a C57BL6/J male mouse model of arterial thrombosis were identified by pathway enrichment and pairwise analyses from the common gene ontology enrichment and dysregulated proteins between carotid and coronary arterial thrombi, and validated by immunohistochemistry.

RESULTS: Spatial proteomics of the coronary arterial thrombi collected from 7 patients with myocardial infarct revealed 7 common dysregulated proteins in 2 cohorts of patients, and upregulation of TGF-β1 (transforming growth factor β1) was the most prominent fibrosis-related protein. Inhibition of TGF-β1 resulted in delayed arterial thrombosis and accelerated blood flow restoration in mouse model. We further expanded the spatial proteomic workflow to the carotid artery thrombi collected from 11 patients with cerebral infarction. Pairwise proteomic analysis of stiff and soft regions between carotid and coronary arterial thrombi further revealed 5 common gene ontology clusters including features of platelet activation, and a common dysregulated protein COL1A1 (collagen type 1 alpha 1) that was reported to be influenced by TGF-β1. We also verified the expression in human and mice carotid arterial thrombi.

CONCLUSIONS: This study demonstrates the spatially distinct composition of proteins in the stiff and soft regions of human arterial thrombi, and suggests that TGF-β1 is a key therapeutic target for promoting arterial thrombolysis.

GRAPHIC ABSTRACT: A graphic abstract is available for this article.

Key Words: microdissection ■ myocardial infarction ■ proteomics ■ thrombectomy ■ thrombosis

Thrombus structure and composition are known as the key factors to influence the thrombolytic efficacy of r-tPA (recombinant tissue-type plasminogen activator) and mechanical thrombectomy.[1–4] In vivo studies in porcines have demonstrated that vessels occluded by fibrin-rich stiff clots require more passes with a Merci Clot Retriever device to achieve recanalization than vessels occluded by erythrocyte-rich soft clots.[5] In addition, the soft clot is more suscepitable to r-tPA-mediated thrombolysis.[5] A clinical study further showed that erythrocyte-rich soft thrombi are associated with more efficient recanalization, and require fewer passes with the stent

Correspondence to: Dan Lu, MD, PhD, Department of Neurology and Stroke Center, The First Affiliated Hospital of Jinan University, Guangzhou, Guangdong 510632, China, Email ludan@jnu.edu.cn or Anding Xu, MD, PhD, Department of Neurology and Stroke Center, The First Affiliated Hospital of Jinan University, Guangzhou, Guangdong 510632, China, Email tlil@jnu.edu.cn or Chi Kwan Tsang, PhD, Clinical Neuroscience Institute, The First Affiliated Hospital of Jinan University, Guangzhou, Guangdong 510632, China, Email tsangch@jnu.edu.cn
*H. Mai, Tianyuan Zhang, and Tao Zhang contributed equally.
Supplemental Material is available at https://www.ahajournals.org/doi/suppl/10.1161/STROKEAHA.123.042486.
For Sources of Funding and Disclosures, see page 1644.

Stroke is available at www.ahajournals.org/journal/str

Nonstandard Abbreviations and Acronyms

ACN	acetonitrile
COL1A1	collagen type 1 alpha 1
GP	glycoprotein
MS	mass spectrometry
PROS1	protein S1
r-tPA	recombinant tissue-type plasminogen activator
SMA	smooth muscle actin
TGF-β1	transforming growth factor β1

retriever.[6] These results suggest that the heterogeneous composition of human thrombi critically influences therapeutic efficacy. Histological studies show that thrombi can generally be characterized into 2 types of tissue compositions: fibrin-rich and platelet-aggregated stiff regions and erythrocyte-rich soft region.[2] However, little is known about the molecular heterogeneity of the stiff and soft regions in human thrombi. Although a few studies have investigated the proteomics of thrombi in some vascular diseases,[7–10] they analyzed the proteomics of bulk thrombus without subdivision based on its soft and stiff spatial structure.[11,12] In this study, we used proteomics strategies[13] combining with laser-captured microdissection to spatially dissect the stiff and soft regions of 2 types of arterial thrombi collected from patients with myocardial or cerebral infarction, aiming to identify potential new therapeutic targets for facilitating arterial thrombolysis.

METHODS

The data that support the findings of this study are available from the corresponding author upon reasonable request.

Patients and Animals Involved in the Study

The Ethics Committees of the First Affiliated Hospital of Jinan University approved the procedures to collect the 2 types of human arterial thrombi after mechanical thrombectomy (12 samples were collected from patients with myocardial infarction, and 13 samples from patients with cerebral infarction; approval ID: KY-2021-025). This study conducted in accordance with the Declaration of Helsinki.[14] The patients were recruited from 2 cohorts, and the baseline characteristics of patients in the 2 cohorts are shown in Tables 1 and 2. In terms of analogies between the 2 cohorts of patients with carotid arterial thrombi, they had the same proportion of patients with atrial fibrillation and diabetes, and they had a comparable mean National Institutes of Health Stroke Scale score at the time of admission. With respect to the differences between the 2 cohorts, the average age in cohort 1 is higher. In addition, the sex combination in cohort 1 and 2 were different. Patients in cohort 2 were more prevalent in having previous stroke/transient ischemic attack, ischemic heart disease, and hypertension. The prevalence of lifestyle including smoking and alcoholism were also more prevalent in cohort 2.

Table 1. Baseline Characteristics of Patients From Whom the Carotid Arterial Thrombi Were Collected

Characteristics	Cohort 1	Cohort 2
Number of patients, n	3	8
Sex (male), n	2	8
Age, y, mean±SD	76±7.5498	59.25±12.578
Previous stroke/TIA, n	0	3
Previous ischemic heart disease, n	0	1
Atrial fibrillation, n	3	2
Coronary disease, n	3	4
Smoking, n	0	5
Alcoholism, n	0	5
Hypertension, n	3	7
Dyslipidemia, n	2	7
Diabetes, n	3	3
NIHSS at admission, mean±SD	16.333±4.1633	15.25±9.6325

Cohort 1 and 2 represent the discovery and validation cohorts, respectively. NIHSS indicates National Institutes of Health Stroke Scale; and TIA, transient ischemic attack.

Regarding the analogies between the 2 cohorts of patients with coronary arterial thrombi, both cohorts had the same proportion of male/female. Additionally, there was no individual with atrial fibrillation in either cohort. The differences between 2 cohorts included average ages, the proportion of patients with previous stroke/transient ischemic attack, ischemic heart disease, and coronary artery disease, which were more prevalent in cohort 2. In addition, patients in cohort 2 with smoking, alcoholism, and dyslipidemia were more prevalent. For spatial proteomics analysis, we used 7 coronary arterial thrombi collected from patients with myocardial infarct (3 patients were recruited in the first cohort and 4 patients in the second cohort) and 11 carotid arterial thrombi from patients with cerebral infarct (3 patients were recruited in the first cohort and 8 patients in the second cohort). The enlarged sample size in the second cohort served as validation for the results from the first cohort. Considering that the variations of handling techniques during sample collection, preparation, and processing would generate significant batch effect, we did not combine the samples from 2 cohorts for proteomics analysis. Thrombi were dissected and divided into stiff and soft parts. We analyzed the matched number of samples in the stiff region versus soft region in all cohorts. In the first cohort of coronary and carotid arterial thrombi, each group contained 3 patients (3 stiff regions versus 3 soft regions). In the second cohorts, 4 patients were included for coronary arterial thrombus samples (4 stiff regions versus 4 soft regions) and 8 patients for the carotid arterial thrombus samples (8 stiff regions versus 8 soft regions). The remaining thrombi from the rest of patients (2 patients with cerebral infarction and 5 patients with myocardial infarction) were used for validation by immunohistochemical staining. This study was conducted following the guidelines[15] for case series. The Institutional Animal Care and Use Committee of Jinan University (approval ID: 20201007-02) approved the mouse experimental protocol. We used C57BL/6J male mice (8–12 weeks old) housed in pathogen-free facilities with 12 hours day and night cycles for the animal experiments in this study. All mice were randomly allocated to treatment groups. In the study, none of the animals were excluded.

Table 2. Baseline Characteristics of Patients From Whom the Coronary Arterial Thrombi Were Collected

Characteristics	Cohort 1	Cohort 2
Number of patients, n	3	4
Sex (male), n	3	4
Age, y, mean±SD	53.33±3.6147	61.75±4.6213
Previous stroke/TIA, n	0	1
Previous ischemic heart disease, n	0	2
Atrial fibrillation, n	0	0
Coronary disease, n	1	4
Smoking, n	1	2
Alcoholism, n	0	1
Hypertension, n	2	3
Dyslipidemia, n	1	3
Diabetes, n	0	1

Cohort 1 and 2 represent the discovery and validation cohorts, respectively. TIA indicates transient ischemic attack.

Retrieval of Thrombi

Solitaire stent retriever was used for mechanical endovascular thrombectomy from the occluded internal carotid or coronary arteries. The thrombi extracted after thrombectomy were kept in 4% neutral-buffered formalin, washed twice with 0.1 mol/L PBS for 15 minutes and cryopreserved overnight with 30% sucrose solution at 4 °C. To avoid the formation of ice crystals, samples were further embedded in optimal cutting temperature compound under the cooled isopentane container placed on dry ice. The samples were stored at −80 °C until cryosectioning.

Laser Capture Microdissection of Soft and Stiff Thrombi

For microdissection of the soft and stiff regions of thrombi, images of the entire Masson-stained slides and sections of interest were acquired using a Leica laser capture microdissection 7000 system. Serial human thrombus sections (10 µm) were adhered to membrane slides (Zeiss, 415190-9041-000) for Masson triple staining. For each sample, the stiff and soft regions of the thrombus sections were selected with a manual closed-shape drawing tool based on the discernible histochemical features of the stiff and soft regions and dissected with a UV laser. The sections were then serially dehydrated with ethanol and air-dried under a fume hood for 15 minutes. We selected soft (red color) and stiff (blue color) regions with clearly identifiable histochemical features by Masson triple staining under view of the microscopy and then cut each region separately in serial sections for a total area of 2 mm^2 for each proteomic sample. The 2 mm^2 area of thrombus samples were collected in the lids of 0.5 ml thermotubes, which were carefully sealed and immediately frozen in liquid nitrogen at the end of the procedure. The dissected samples in the thermotubes were stored at −80 °C until use. Protein extraction from the samples were performed by resuspending samples in 8 mol/L urea containing 10 mmol/L Tris-HCl, pH 8.5, and protein contents were determined by spectrophotometer using fluorescence emission from tryptophan (excitation 280 nm, emission 350 nm).

Sample Peptides Preparation

Samples were rehydrated with serial dilution of ethanol (100%, 75%, 50%), and basic hydrolysis was performed by heating samples to 95 °C for 30 minutes in a thermo-mixer (mass spectrometry [MS], −100) in 0.1 mol/L Tris-HCl (pH 10). Next, samples were resuspended for denaturation in 30 µL lysis buffer (6 mol/L urea, 2 mol/L thiourea, 100 m mol/L ammonium bicarbonate) in the pressure cycling technology-MicroPestle device. Samples were then placed in a Barocycler (PressureBioSciences Inc, NEP2320-45k) with on and off at 45 000 psi for 30 seconds at high pressure and 10 seconds at ambient pressure for 90 cycles. For reduction and alkylation, open pressure cycling technology-MicroPestles were added with 10 uL of 100 mmol/L Tris (2-carboxyethyl) phosphine and 2.5 uL of 800 mmol/L iodoacetamide incubated in dark for 30 minutes under gentle vortexing (800 rpm) on a Thermo Shaker at 25 °C. For digestion, Lys-C was added to the lysate at a 1:80 (weight/weight) ratio of enzyme to substrate. Pressure cycle was then applied in the sample holder with the Lys-C digestion scheme for 45 cycles. Then trypsin was added at a ratio of 1:20 (weight/weight) of enzyme to substrate in the lysate solution. The pressure cycle was applied to the samples with the trypsin digestion scheme for 120 cycles. To stop digestion, the peptides were acidified to pH 2 to 3 with 1% trifluoroacetic acid in 99% isopropanol at a ratio of 1:1 v/v. The peptides were treated in SOLAµ solid phase extraction plates (Thermo Fisher ScientificTM, San Jose, United States) for desalting, and the dried peptides were reconstituted in 10 µL 2% acetonitrile/0.1% trifluoroacetic acid and subjected to Pierce Quantitative Colorimetric Peptide Assay for quantification.

Liquid Chromatography and MS Analysis

Mass spectrometry was performed by a nanoElute UHPLC (Bruker Daltonics, Germany) coupled to a timsTOF Pro (Bruker Daltonics, Germany) equipped with a CaptiveSpray ion source. Peptide powder was reconstituted in buffer A (0.1% formic acid in water). Peptide digest were separated at a flow rate of 300 nL/min using 60 minutes gradient on a 15 cm analytical column (75 µm inner diameter, 1.9 µm particle size, C18 beads) with an integrated Toaster column oven at 50 °C. The mobile phase B was eluted with 0.1% formic acid in acetonitrile. Phase B was increased from 5% to 27% in 50 minutes, 27% to 40% in 10 minutes, 40% to 80% in 2 minutes, and was sustained at 80% for 3 minutes. The timsTOF Pro was operated in a positive ion data-dependent acquisition Parallel Accumulation Serial Fragmentation mode. The capillary voltage was set to 1400 V. The MS and MS/MS spectra were acquired from 100 to 1700 m/z, and an ion mobility range (1/K0) from 0.7 to 1.3 Vs/cm^2. The ramp and accumulation time were set to 100 ms to achieve a duty cycle close to 100%. To perform diaPASEF acquisition mode, we defined one 28 Th isolation window from m/z 384 to 1059. This method was modified based on the method reported previously.[16]

Mouse Artery Thrombosis Model and Imaging Analysis for Blood Flow

Mouse thrombosis model was performed by 10% Ferric chloride (Macklin Catalog No. I811935) as previously described (Supplemental Methods).[17] For inhibition of TGF-β1

 Stroke. 2023;54:1636–1644. DOI: 10.1161/STROKEAHA.123.042486

(transforming growth factor β1), SB525334 (Absin Catalog No. abs810374; 20 mg/kg, a blood concentration of 34.3 mg/mL) was administered via the tail vein 30 minutes before and after ferric chloride treatment and control group was treated with equal volume of saline. During the ferric chloride-induced thrombosis in carotid artery, continuous recording of blood flow in the mouse carotid artery for 15 minutes and images of blood perfusion in mice were acquired using the PeriCam PSI system. For TGF-β1 inhibitor in combination with the r-tPA for thrombolysis analysis, TGF-β1 inhibitor with or without r-tPA (0.9 mg/kg, Actilyse, Boehringer Ingelheim Pharma GmbH & Co, United Kingdom) was administered via the tail vein after cervical artery occlusion. Continuous recording of mice carotid artery blood flow for 180 minutes was performed, and images of blood perfusion in mice were acquired using PeriCam PSI system. GraphPad Prism (version 8.0) software was used for statistical analysis.

Immunohistochemical Analysis

Human and mouse thrombi were fixed in 4% phosphate-buffered formaldehyde, and 10 μm thick of frozen sections were prepared for immunohistochemical analysis. Human thrombi were stained with Masson stain (Wanleibio WLA045a) and examined with laser-captured microdissection. Anti-TGF-β1 (Abcam Catalog No. 99562), anti-COL1A1 (collagen type I alpha 1 chain, Abcam Catalog No. ab279711), anti-Vimentin (Invitrogen Catalog No. Pa5-27231), and anti-SMA (smooth muscle actin, Thermofisher Catalog No. 53-9760-80) antibodies were used for immunofluorescence analysis.

Statistical Analysis

Statistical analysis was performed using R (version 3.6.3). Log_2 fold-change was calculated from the mean ratio of protein expression. Student *t* test was performed for each pair of groups to be compared. Adjusted *P* values were calculated using the Benjamini–Hochberg correction. The criterion for selecting dysregulated (either upregulated or downregulated) proteins which differentially expressed in the stiff-region compared with those in soft region was based on the *P* value with <0.05 and fold-change >1.3. Gene ontology pathway enrichment analysis was performed using Goplot (version 1.0.2). Additional plots were generated using the ggplot2 (version 3.3.3) and ComplexHeatmap (version 2.4.3) packages. *P*<0.05 were considered statistically significant. Experimental animal group assignment was randomized using a 4-digit lottery draw, and the assignment process was performed covertly. The operators for measurements and analyses were blinded to avoid possible bias. An online calculator (https://www.trialstats.com/sample-size/4/) with prespecified criteria, including SD and averages from historical and preliminary data, was used to determine sample size, with a significance level of 0.05 and power of 0.8. For experiments with 2 groups, either a paired *t* test was used depending on the type of data. To ensure unbiased results, proteomics data were analyzed in which sample group inner diameters were reassigned, and technicians were unaware of the true identity of the samples, and data analysis was performed by a separate person using R software with predefined protocols. Immunostaining quantification data were analyzed by a separate individual who was unaware of the TGF-β1 inhibitor treatment and control groups and the identity of the samples. Data were analyzed twice for accuracy and consistency. Mouse blood flow quantification data were collected by an individual who was unaware of group assignment and analyzed by a statistician who was also unaware of group assignment.

RESULTS

To test the hypothesis that spatial proteomics analysis of soft and stiff regions in acute human thrombus biopsies would provide new insights into therapeutic targets against thrombosis, we first dissected soft and stiff regions of human coronary arterial thrombi collected from patients with myocardial infarction. We employed laser-captured microdissection to spatially and specifically dissect the Masson trichrome-positive fibrin-rich region (stiff region) and fibrin-deficient region (soft region) of thrombus biopsies as shown in the workflow (Figure 1A; Figure S1). To increase the statistical power of proteomics analysis, we performed 2 independent cohorts and compared the dysregulated proteins (*P* value with <0.05 and fold-change >1.3) in coronary arterial thrombi collected from the first cohort (3 patients) and those from the second cohort (4 patients). After comparing the stiff with soft regions of coronary arterial thrombi, we compared the dysregulated proteins between the 2 cohorts of patients. We identified 7 common dysregulated proteins, including 4 upregulated proteins (MTHFD1 [methylenetetrahydrofolate dehydrogenase, cyclohydrolase and formyltetrahydrofolate synthetase 1], TGF-β1, H1-3 [histone cluster 1 H1 family member 3], and COL1A1) and 3 downregulated proteins (APCS [amyloid p component, serum], PROS1 [protein S1], and ATP5F1D [ATP synthase F1 subunit delta]; Figure 1B; Tables S1 and S2). Given that TGF-β1 is among the prominent upregulated proteins and it is closely related with fibrosis, we further validated TGF-β1 expression in human coronary artery thrombi. Immunofluorescence staining revealed a higher percentage of TGF-β1 positive cells in fibroblasts (vimentin+) than that in total cells (Figure 1C). Next, we investigated the role of TGF-β1 in arterial thrombus formation by using a well-established mouse model of $FeCl_3$-induced thrombosis (Figure 1D). We performed a functional assay and showed that the average first clotting time after administration of TGF-β1 inhibitor was significantly longer than that in the saline control group (412 versus 151 seconds; Figure 1D and 1E). In addition, the mean time of final vessel occlusion in the TGF-β1 inhibitor-treated group was 270 seconds longer than that in the saline control group (Figure 1D and 1E). To examine the role of TGF-β1 in a more clinically relevant scenario, we treated the mice with TGF-β1 inhibitor in combination with r-tPA after thrombus formation. Based on our results, we found that treatment with a combination of r-tPA and TGF-β1 inhibitor (mean 76.03%, at the 3-hour time point compared with baseline) resulted in a significant increase in blood flow compared with

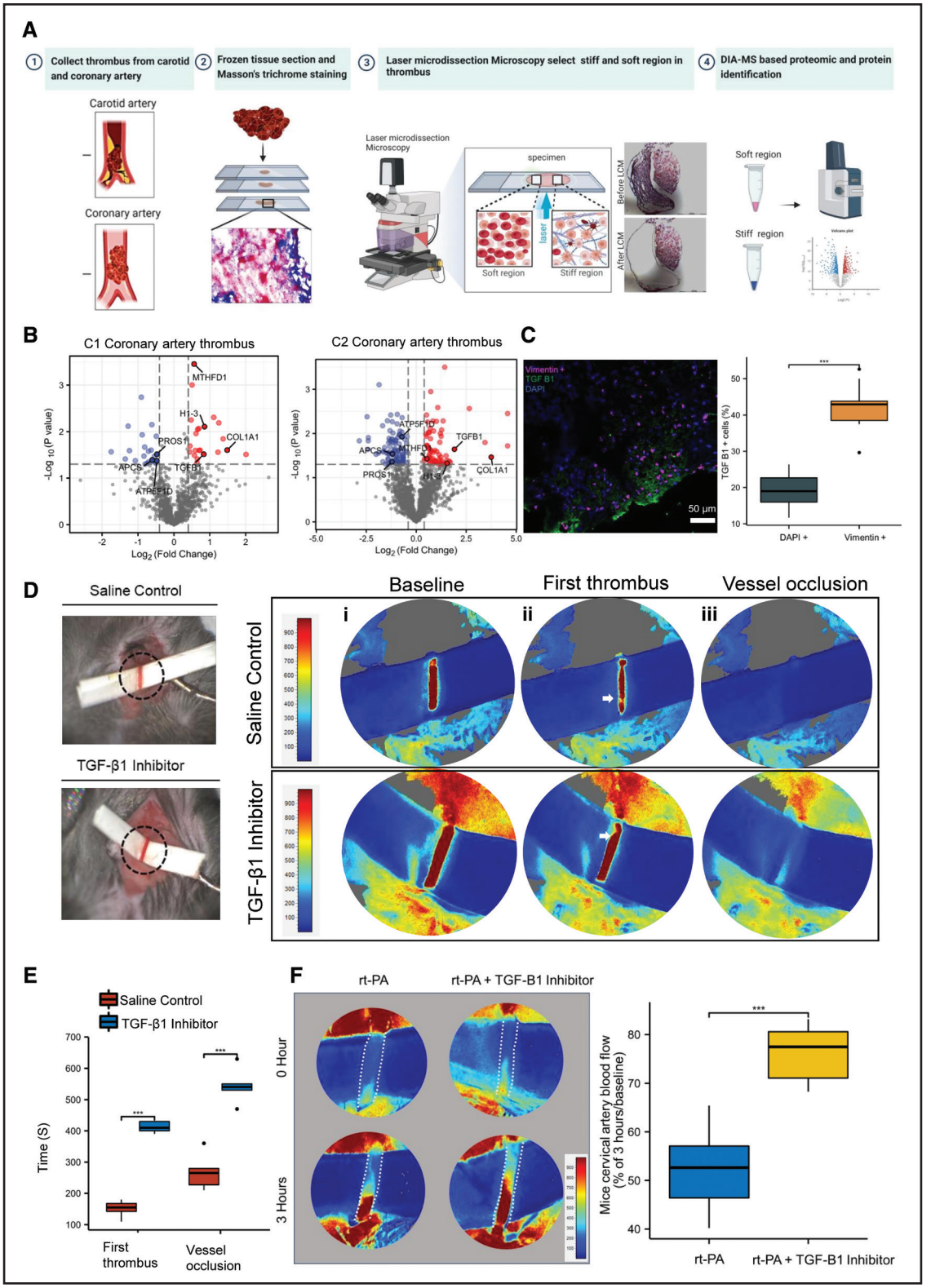

Figure 1. Spatial proteomics reveals signature of coronary artery-derived thrombus in stiff regions compared with soft regions. **A**, Proteomic analysis workflow for human artery-derived thrombi. Biopsies were stained with Masson trichrome for stiff regions (blue) and soft regions (red), which were then selected for data-independent acquisition mass spectrometry (DIA–MS) proteomic analysis under laser capture microdissertion microscopy. **B**, The volcano plots showing the common dysregulated proteins identified from stiff and soft regions in the 2 cohorts of coronary arterial thrombi collected from patients with myocardial infarction. C1 represents cohort 1 and C2 represents cohort 2. **C**, Representative image showing TGF (transforming growth factor)-β1 and fibroblast (vimentin+) stainning in the human coronary artery thrombus. **Right**, the quantification of percentage of TGF-β1 positive cells in the vimentin-positive cells and DAPI (4′,6-diamidino-2-phenylindole)-positive cells (n=5). (*Continued*)

treatment with r-tPA alone (mean 52.17%, at the 3-hour time point compared with baseline; Figure 1F).

We further extended the scope of this study by performing spatial proteomics analysis in the carotid arterial thrombi collected from 11 patients with cerebral infarction (Tables S3 and S4). We then integrated the differentially expressed proteins identified from the 2 types of artery thrombi into biological process analysis. Gene ontology enrichment pathway analysis in the first cohort revealed 85 and 284 clusters in the carotid and coronary artery-derived thrombi, respectively. In the second cohort, there were 401 and 362 clusters were identified in the carotid and coronary artery-derived thrombi, respectively (Figure 2A). Interestingly, there were 5 gene ontology enrichment clusters commonly found in the 2 types of artery-derived thrombi from the 2 cohorts (Figure 2B). Intriguingly, they were associated with platelet activation (platelet alpha granules), cytoplasmic vesicle and lumen, and cellular releasing mechanisms (secretory granule lumen, vesicle lumen, and platelet alpha granule lumen; Figure 2C through 2F). Our findings are consistent with the previous studies reporting that platelets are the major component in the stiff region of thrombi that release TGF-β1 during activation.[18,19] In addition to TGF-β1, we found that COL1A1 was the other prominent dysregulated protein shared between carotid and coronary arterial thrombi in the 2 cohorts (Figure 3A and 3B). Interestingly, TGF-β has been reported to stimulate COL1A1 expression in mouse cholangiocytes.[20] We also found that COL1A1 was upregulated in both coronary and carotid arterial thrombi (Figure 3B), with an average expression of 1.7-fold increase in the stiff thrombus region compared with that in soft region in the first cohort (Figure 3C), whereas there was an average of 2.3-fold increase in the second cohort (Figure 3D). Furthermore, we verified by immunofluorescence staining that COL1A1 proteins were expressed in the stiff region of arterial thrombi collected from patients (Figure 3E). Finally, we performed SMA-immunofluorescence staining for visualization of arterial smooth muscle cells demarcating the vessel wall, and verified that COL1A1 was assembled in the thrombi at the lumen of mouse carotid artery (Figure 3F).

DISCUSSION

Using spatially distinct proteomics analysis in the soft and stiff regions of arterial thrombi, this study provides a new perspective on the molecular landscape of the fibrin-rich stiff and erythrocyte-rich soft regions of human thrombus biopsies. We demonstrate that inhibition of TGF-β1 significantly prolongs the time of thrombosis and enhances restoration of blood flow in the presence of r-tPA. Furthermore, we found that COL1A1 expression is upregulated in the stiff regions of coronary and carotid arterial thrombi compared with the soft regions,[20] which is in agreement with a recent report showing that TGF-β1 transiently induces type 1 collagen production in mouse cholangiocytes.[21] These observations suggest that TGF-β1 is a potentially promising therapeutic target for slowing down the process of stiffening in acute arterial thrombi. In addition, it would be interesting to investigate in the future whether therapeutic inhibition of TGF-β1 and COL1A1 would extend the time window for acute ischemic stroke.

With respect to the proteomic gene ontology pathway analysis in stiff and soft regions, we found that platelet activation may be an important molecular process for both coronary and carotid arterial thrombosis. It has been reported that platelets are mechanosensitive to rigidity of thrombus substrate that promotes platelet adhesion and spreading, resulting in enhanced platelet activation.[22] Platelets might interact with collagen through their receptors with GP (glycoprotein) Ib/V/IX as previously reported.[23] Whether targeting GP Ib/V/IX can prevent platelet activation in the stiff regions of the thrombus and change the composition of the thrombus await future study. In addition, platelet activation promotes inflammation which contributes to the interaction of platelets with endothelial cells and neutrophils. Consistent with this idea, it has been reported that neutrophil activation[24] and neutrophil extracellular traps[25] can enhance thrombus formation and thus they may contribute to resistance to reperfusion therapy.

In addition to TGF-β1 and COL1A1, we identified other potentially important targets from the 2 cohorts of arterial thrombus analysis. For example, we found that PROS1 was downregulated in both coronary arterial thrombi in the stiff region compared with that in soft region (Figures 1B and 3B). It has been recently reported that PROS1 is a pleiotropic factor with antithrombotic[26] and immunomodulatory properties. Thus, we speculate that PROS1 may regulate coagulation and thrombosis in patients with COVID-19 who have been reported to show symptoms with cardiac infarction.[27] Further work is required to confirm the therapeutic effect of targeting PROS1 on antithrombosis and prevention of cardiac vascular diseases in patients with long COVID-19.

A limitation of this study is our small sample size. Larger independent cohorts from different centers and

Figure 1 Continued. D, Representative images of mouse arterial thrombus formation model induced by 10% $FeCl_3$ for vascular injury in saline control group (**upper**) or TGF-β1 inhibitor-treated group (**lower**). **Right**, the representative laser speckle contrast images (LSCI) at baseline (i), first thrombus formation (as indicated by the arrow) (ii), and vessel occlusion (iii). **E**, Statistical analysis of the time spent in the $FeCl_3$-induced first thrombus and vessel occlusion in mouse artery of untreated (n=6) and TGF-β1 inhibitor-treated (n=5) mice. **F**, Representative LSCI images of r-tPA and r-tPA (recombinant tissue-type plasminogen activator) combined with TGF-β1 inhibitor treatment in mice vessel occlusion (dash line) at time points of 0 h and 3 h. **Right**, Quantification of mouse cervical arterial blood flow relative to the basal level after treatment with r-tPA (n=7) and r-tPA combined with TGF-β1 inhibitor (n=7) for 3 h. Data are expressed as mean±SEM. COL1A1 indicates collagen type 1 alpha 1; and PROS1, protein S1. ***P<0.001.

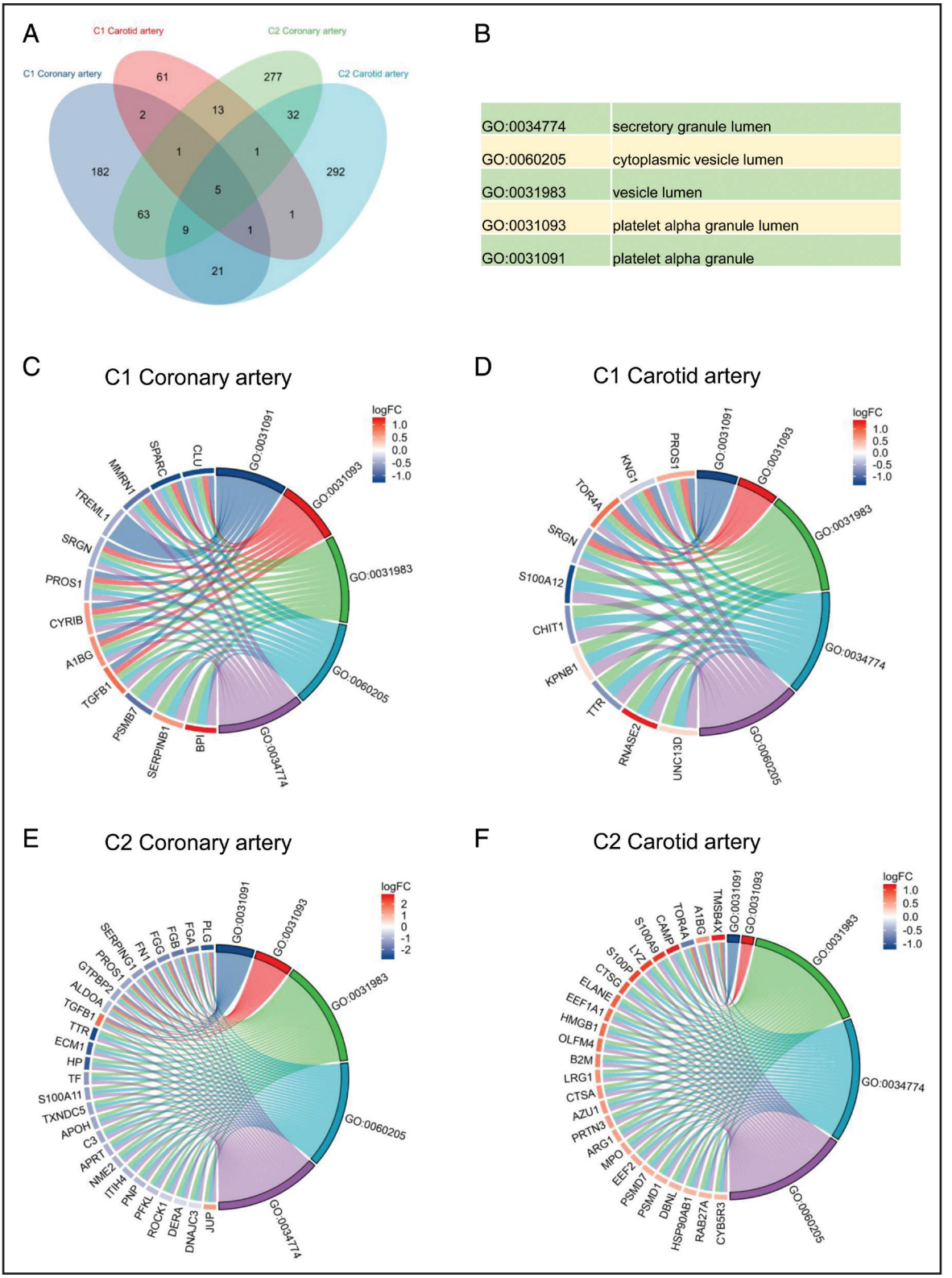

Figure 2. Pair-wise spatial proteomic analyses of carotid and coronary artery-derived thrombi reveal signature genes and pathways. **A**, Venn diagram showing the numbers of common and unique gene ontology (GO) clusters in the carotid and coronary arterial thrombi from 2 cohorts. C1 represents cohort 1 and C2 represents cohort 2. **B**, Identification numbers and the corresponding names of the identified GO clusters. **C** through **F**, Chord diagrams showing the enriched common GO clusters of dysregulated proteins in the thrombus proteomics between stiff and soft regions in carotid and coronary artery-derived thrombi in the 2 cohorts. Cutoff for dysregulated proteins were set at $P<0.05$ and fold-change (FC) >1.3. Enriched GO clusters are shown on the right side, and genes contributing to the corresponding enrichment are shown on the left side of the diagrams. Length of the brick for each protein corresponds to the sum of $|\log_2(FC)|$ in multiple enriched GO clusters. Length of the brick for each enriched GO cluster corresponds to the sum of $|\log_2(FC)|$ in one or more proteins. C1 represents cohort 1 and C2 represents cohort 2.

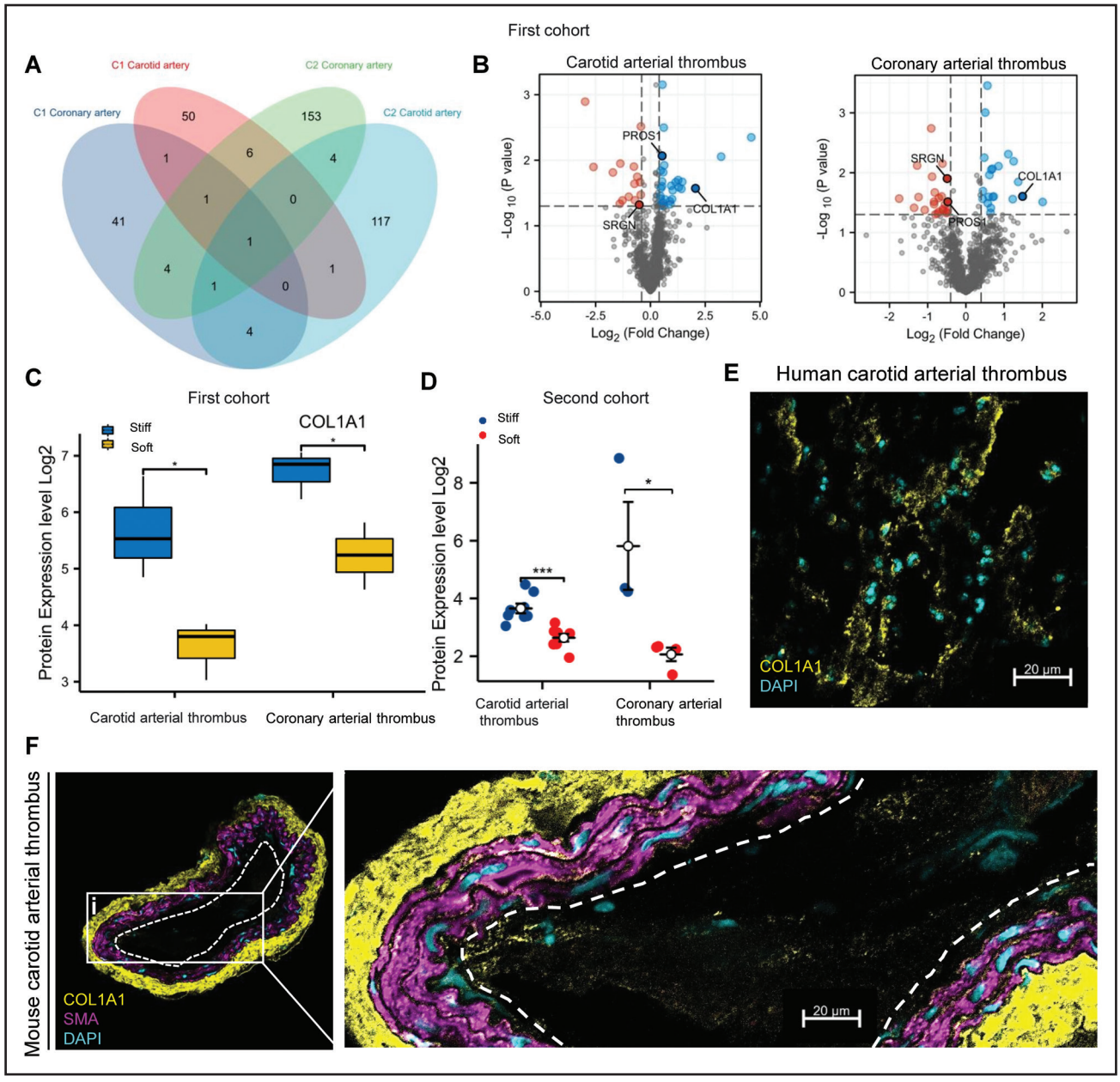

Figure 3. Spatial proteomics reveals a common upregulated protein from carotid and coronary arterial thrombi.
A, Venn diagram showing the numbers of common and unique dysregulated proteins in the stiff regions compared with those in the soft regions from the carotid and coronary arterial thrombi in 2 cohorts. **B**, Volcano plots comparing the down-(red) and upregulation (blue) of proteins in carotid and coronary arterial thrombi in the first cohort. **C** and **D**, Human thrombus proteomic protein expression of COL1A1 (collagen type 1 alpha 1) in carotid and coronary arterial thrombi. The *y* axis indicates the protein expression ratio determined by DIA-based quantitative proteomics in the first cohort (**C**) and second cohort (**D**). **E**, Representative image validating the COL1A1 staining in human carotid arterial thrombus. **F**, Immunofluorescence image showing the localization of COL1A1 (yellow), SMA (magenta) and DAPI ([4′,6-diamidino-2-phenylindole]; cyan) in the thrombus (dash line) located at the lumen side of mouse carotid artery. **Right**, Enlarged image of the boxed region. Pair-wise comparisons between the stiff and soft regions were performed using Student *t* test. The cutoff was set at fold-change >1.3 and $P<0.05$. Data are expressed as mean±SEM. PROS1 indicates protein S1; SMA, smooth muscle actin; and SRGN, serglycin. *$P<0.05$, ***$P<0.001$.

countries would allow stronger correlation analysis with clinical variables and molecular characterization. Finally, further studies on the molecular relationship between stiff and soft regions compared with arterial and venous thrombi would be important to prevent the chronic thrombus formation and progression.[28] In addition, detailed spatial proteomics studies of other cellular thrombus compositions such a leukocytes and endothelial cells would be necessary to improve the treatment and clinical outcomes of thrombosis-related diseases.

ARTICLE INFORMATION

Received September 13, 2022; final revision received March 14, 2023; accepted March 21, 2023.

Affiliations

Department of Neurology and Stroke Center (H.M., Tianyuan Zhang, A.L., B.Y., N.H., X.L., A.X., D.L.), Clinical Neuroscience Institute (H.M., Tianyuan Zhang, A.L., X.L., C.K.T., A.X., D.L.), Department of Cardiology (Tao Zhang), and Department of Neurology (Z.W., X.L.), The First Affiliated Hospital of Jinan University, Guangzhou, China. Munich Medical Research School (MMRS), Ludwig-Maximilians University Munich, Germany (H.M.). Insititute for Tissue Engineering and Regenerative Medicine (iTERM), Helmholtz Zentrum München, Germany (H.M.).

Acknowledgments

This work was supported by grants from the National Natural Science Foundation of China (81801150, 81971121, 82171316, 81671167, and 81974210), the Science and Technology Planning Project of Guangdong Province, China (2017A020215049, 2019A050513005, 2020A0505100045), Natural Science Foundation of Guangdong Province (2018A0303130182, 2020A1515010279, and 2022A1515012311), the Fundamental Research Funds for the Central Universities (21621102), and Science and Technology Program of Guangzhou, China (2014Y2-00505 and 201508020004). T.Y.Z was supported by the Outstanding Innovative Talents Cultivation Funded Programs for Doctoral Students of Jinan University (2021CXB011). Workflow illustration is created by BioRender.com. We acknowledge P.W.F and L.S.D for discussion of the clinical baseline characteristic data of patients. Drs Lu, Xu, and Tsang conceived the study, designed experiments, and write the final article; Dr Mai and T.Y.Z performed experiments and write the first draft of article; T.Z. and Dr Yang provided human samples and involve in data analysis; Drs Wu, Liu, Lu, and He performed experiments, and analyzed the data; all authors contributed to article final preparation.

Sources of Funding

None.

Disclosures

None.

Supplemental Material

Supplemental Methods
Figure S1
Tables S1–S4

REFERENCES

1. Chueh JY, Wakhloo AK, Hendricks GH, Silva CF, Weaver JP, Gounis MJ. Mechanical characterization of thromboemboli in acute ischemic stroke and laboratory embolus analogs. *AJNR Am J Neuroradiol*. 2011;32:1237–1244. doi: 10.3174/ajnr.A2485
2. Alkarithi G, Duval C, Shi Y, Macrae FL, Ariens RAS. Thrombus structural composition in cardiovascular disease. *Arterioscler Thromb Vasc Biol*. 2021;41:2370–2383. doi: 10.1161/ATVBAHA.120.315754
3. Mercado-Shekhar KP, Kleven RT, Aponte Rivera H, Lewis R, Karani KB, Vos HJ, Abruzzo TA, Haworth KJ, Holland CK. Effect of clot stiffness on recombinant tissue plasminogen activator lytic susceptibility in vitro. *Ultrasound Med Biol*. 2018;44:2710–2727. doi: 10.1016/j.ultrasmedbio.2018.08.005
4. Jolugbo P, Ariens RAS. Thrombus composition and efficacy of thrombolysis and thrombectomy in acute ischemic stroke. *Stroke*. 2021;52:1131–1142. doi: 10.1161/STROKEAHA.120.032810
5. Yuki I, Kan I, Vinters HV, Kim RH, Golshan A, Vinuela FA, Sayre JW, Murayama Y, Vinuela F. The impact of thromboemboli histology on the performance of a mechanical thrombectomy device. *AJNR Am J Neuroradiol*. 2012;33:643–648. doi: 10.3174/ajnr.A2842
6. Maekawa K, Shibata M, Nakajima H, Mizutani A, Kitano Y, Seguchi M, Yamasaki M, Kobayashi K, Sano T, Mori G, et al. Erythrocyte-rich thrombus is associated with reduced number of maneuvers and procedure time in patients with acute ischemic stroke undergoing mechanical thrombectomy. *Cerebrovasc Dis Extra*. 2018;8:39–49. doi: 10.1159/000486042
7. Rossi R, Mereuta OM, Barbachan ESM, Molina Gil S, Douglas A, Pandit A, Gilvarry M, McCarthy R, O'Connell S, Tierney C, et al. Potential biomarkers of acute ischemic stroke etiology revealed by mass spectrometry-based proteomic characterization of formalin-fixed paraffin-embedded blood clots. *Front Neurol*. 2022;13:854846. doi: 10.3389/fneur.2022.854846
8. Munoz R, Santamaria E, Rubio I, Ausin K, Ostolaza A, Labarga A, Roldan M, Zandio B, Mayor S, Bermejo R, et al. Mass spectrometry-based proteomic profiling of thrombotic material obtained by endovascular thrombectomy in patients with ischemic stroke. *Int J Mol Sci*. 2018;19:498. doi: 10.3390/ijms19020498
9. Dargazanli C, Zub E, Deverdun J, Decourcelle M, de Bock F, Labreuche J, Lefevre PH, Gascou G, Derraz I, Riquelme Bareiro C, et al. Machine learning analysis of the cerebrovascular thrombi proteome in human ischemic stroke: an exploratory study. *Front Neurol*. 2020;11:575376. doi: 10.3389/fneur.2020.575376
10. Han B, Li C, Li H, Li Y, Luo X, Liu Y, Zhang J, Zhang Z, Yu X, Zhai Z, et al. Discovery of plasma biomarkers with data-independent acquisition mass spectrometry and antibody microarray for diagnosis and risk stratification of pulmonary embolism. *J Thromb Haemost*. 2021;19:1738–1751. doi: 10.1111/jth.15324
11. Hochrainer K, Yang W. Stroke proteomics: from discovery to diagnostic and therapeutic applications. *Circ Res*. 2022;130:1145–1166. doi: 10.1161/CIRCRESAHA.122.320110
12. Suissa L, Guigonis JM, Graslin F, Robinet-Borgomano E, Chau Y, Sedat J, Lindenthal S, Pourcher T. Combined omic analyzes of cerebral thrombi: a new molecular approach to identify cardioembolic stroke origin. *Stroke*. 2021;52:2892–2901. doi: 10.1161/STROKEAHA.120.032129
13. Eckert MA, Coscia F, Chryplewicz A, Chang JW, Hernandez KM, Pan S, Tienda SM, Nahotko DA, Li G, Blazenovic I, et al. Proteomics reveals NNMT as a master metabolic regulator of cancer-associated fibroblasts. *Nature*. 2019;569:723–728. doi: 10.1038/s41586-019-1173-8
14. World Medical A. World Medical Association Declaration of Helsinki: ethical principles for medical research involving human subjects. *JAMA*. 2013;310:2191–2194. doi: 10.1001/jama.2013.281053
15. Kempen JH. Appropriate use and reporting of uncontrolled case series in the medical literature. *Am J Ophthalmol*. 2011;151:7–10.e1. doi: 10.1016/j.ajo.2010.08.047
16. Meier F, Brunner AD, Frank M, Ha A, Bludau I, Voytik E, Kaspar-Schoenefeld S, Lubeck M, Raether O, Bache N, et al. diaPASEF: parallel accumulation-serial fragmentation combined with data-independent acquisition. *Nat Methods*. 2020;17:1229–1236. doi: 10.1038/s41592-020-00998-0
17. Covarrubias R, Chepurko E, Reynolds A, Huttinger ZM, Huttinger R, Stanfill K, Wheeler DG, Novitskaya T, Robson SC, Dwyer KM, et al. Role of the CD39/CD73 purinergic pathway in modulating arterial thrombosis in mice. *Arterioscler Thromb Vasc Biol*. 2016;36:1809–1820. doi: 10.1161/ATVBAHA.116.307374
18. Meyer A, Wang W, Qu J, Croft L, Degen JL, Coller BS, Ahamed J. Platelet TGF-beta1 contributions to plasma TGF-beta1, cardiac fibrosis, and systolic dysfunction in a mouse model of pressure overload. *Blood*. 2012;119:1064–1074. doi: 10.1182/blood-2011-09-377648
19. Grainger DJ, Wakefield L, Bethell HW, Farndale RW, Metcalfe JC. Release and activation of platelet latent TGF-beta in blood clots during dissolution with plasmin. *Nat Med*. 1995;1:932–937. doi: 10.1038/nm0995-932
20. Feitsma LJ, Brondijk HC, Jarvis GE, Hagemans D, Bihan D, Jerah N, Versteeg M, Farndale RW, Huizinga EG. Structural insights into collagen binding by platelet receptor glycoprotein VI. *Blood*. 2022;139:3087–3098. doi: 10.1182/blood.2021013614
21. Liu J, Eischeid AN, Chen XM. Col1A1 production and apoptotic resistance in TGF-beta1-induced epithelial-to-mesenchymal transition-like phenotype of 603B cells. *PLoS One*. 2012;7:e51371. doi: 10.1371/journal.pone.0051371
22. Qiu Y, Brown AC, Myers DR, Sakurai Y, Mannino RG, Tran R, Ahn B, Hardy ET, Kee MF, Kumar S, et al. Platelet mechanosensing of substrate stiffness during clot formation mediates adhesion, spreading, and activation. *Proc Natl Acad Sci U S A*. 2014;111:14430–14435. doi: 10.1073/pnas.1322917111
23. Wichaiyo S, Parichatikanond W, Rattanavipanon W. Glenzocimab: a GPVI (Glycoprotein VI)-targeted potential antiplatelet agent for the treatment of acute ischemic stroke. *Stroke*. 2022;53:3506–3513. doi: 10.1161/STROKEAHA.122.039790
24. Nouboussie DF, Reeves BN, Strahl BD, Key NS. Neutrophils: back in the thrombosis spotlight. *Blood*. 2019;133:2186–2197. doi: 10.1182/blood-2018-10-862243
25. Ducroux C, Di Meglio L, Loyau S, Delbosc S, Boisseau W, Deschildre C, Ben Maacha M, Blanc R, Redjem H, Ciccio G, et al. Thrombus neutrophil extracellular traps content impair tPA-induced thrombolysis in acute ischemic stroke. *Stroke*. 2018;49:754–757. doi: 10.1161/STROKEAHA.117.019896
26. Heeb MJ, Gandrille S, Fernandez JA, Griffin JH, Fedullo PF. Late onset thrombosis in a case of severe protein S deficiency due to compound heterozygosity for PROS1 mutations. *J Thromb Haemost*. 2008;6:1235–1237. doi: 10.1111/j.1538-7836.2008.02994.x
27. Lemke G, Silverman GJ. Blood clots and TAM receptor signalling in COVID-19 pathogenesis. *Nat Rev Immunol*. 2020;20:395–396. doi: 10.1038/s41577-020-0354-x
28. Broderick JP, Hill MD. Advances in acute stroke treatment 2020. *Stroke*. 2021;52:729–734. doi: 10.1161/STROKEAHA.120.033744